Inorg. Chem. **2007**, *46*, 6933–6941

$REAu_2In_4$ (RE = La, Ce, Pr, Nd): Polyindides from Liquid Indium

James R. Salvador,[†] Khang Hoang,[‡] S. D. Mahanti,[‡] and Mercouri G. Kanatzidis*[,†]

Department of Chemistry, Michigan State University, East Lansing, Michigan 48824, and Department of Physics and Astronomy, Michigan State University, East Lansing, Michigan 48824

Received April 3, 2007

The series of compounds $REAu_2In_4$ (RE = La, Ce, Pr, Nd) crystallize from excess In as rod-shaped single crystals. All members adopt the orthorhombic space group *Pnma* with $a = 18.506(2)$ Å, $b = 4.6865(6)$ Å, and $c = 7.3414(9)$ Å for $LaAu_2In_4$, $a = 18.514(3)$ Å, $b = 4.6624(8)$ Å, and $c = 7.389(1)$ Å for $CeAu_2In_4$, $a = 18.420(4)$ Å, $b = 4.6202(9)$ Å, and $c = 7.376(2)$ Å for the Pr analogue, and $a = 18.406(2)$ Å, $b = 4.6114(5)$ Å, and $c = 7.4073(7)$ Å for $NdAu_2In_4$. The $REAu_2In_4$ series can be regarded as polar intermetallic phases composed of a complex $[Au_2In_4]^{3-}$ polyanion network in which the rare-earth ions are embedded. The $[Au_2In_4]^{3-}$ network features In tetramer units, which defines the compounds as polyindides. Magnetic measurements found no magnetic ordering down to 2 K for any of the compounds. In addition, $LaAu_2In_4$ was found to be Pauli paramagnetic with a small susceptibility. Ab initio density functional methods were used to carry out electronic structure calculations to explore the bonding, the role of gold, and the contributions of different atoms to the density of states near the Fermi energy. We find that the density of states decreases slowly near E_f and reaches a minimum at about 0.5 eV above E_f.

Introduction

Investigations into the ternary phase diagram of rare earth/gold/indium have yielded numerous phases and structures including EuAuIn,[1−3] $REAu_2In$ (RE = Tb−Lu),[4,5] RE_2Au_2In (RE = La−Gd), and RE_2Au_2In (RE = Tm−Lu), which adopt the U_3Si_2 and Zr_3Al_2 structure types respectively based on the rare-earth (RE) atom used.[5] More indium-rich examples have also been found such as $La_3Au_4In_7$,[6] $RE_2Au_3In_5$ (RE = Ce, Pr, Nd, Sm),[7] $Eu_2Au_3In_4$,[8] $YbAuIn_2$,[7] and $EuAuIn_2$.[9] There have been several examples of indium-rich compounds that display heavy fermion behavior, for example, Ce_2MIn_8 (M = Rh, Ir).[10,11] The Ce_nMIn_{3n+2} compounds (n = 1, 2; M = Co, Ir) were found to be both superconducting and heavy fermion compounds.[11] The discovery of such phases and their exotic properties helps drive the exploratory synthesis of Ce/TM/In (TM is a first-, second-, or third-row transition metal) systems. Efforts to produce Ce/TM/In and other RE/TM/In phases as well as the incorporation of other 4d and 5d metals have yielded a multitude of compounds over the last several years, which have further spurred the exploratory work.[12−24]

* To whom correspondence should be addressed. Current address: Department of Chemistry, Northwestern University, 2145 Sheridan Road, Evanston, IL 60208. E-mail: m-kanatzidis@northwestern.edu.
[†] Department of Chemistry, Michigan State University.
[‡] Department of Physics and Astronomy, Michigan State University.

(1) Rossi, D.; Ferro, R.; Contardi, V.; Marazza, R. *Z. Metallkd.* **1977**, *68* (7), 493−494.
(2) Pottgen, R. *J. Mater. Chem.* **1996**, *6* (1), 63−67.
(3) Mullmann, R.; Mosel, B. D.; Eckert, H.; Kotzyba, G.; Pottgen, R. *J. Solid State Chem.* **1998**, *137* (1), 174−180.
(4) Besnus, M. J.; Kappler, J. P.; Meyer, A.; Sereni, J.; Siaud, E.; Lahiouel, R.; Pierre, J. *Physica B & C* **1985**, *130* (1−3), 240−242.
(5) Pottgen, R. *Z. Naturforsch., B:Chem. Sci.* **1994**, *49* (11), 1525−1530.
(6) Galadzhun, Y. V.; Zaremba, V. I.; Kalychak, Y. M.; Hoffmann, R. D.; Pottgen, R. *Z. Anorg. Allg. Chem.* **2000**, *626* (8), 1773−1777.
(7) Galadzhun, Y. V.; Hoffmann, R. D.; Kotzyba, G.; Kunnen, B.; Pottgen, R. *Eur. J. Inorg. Chem.* **1999**, (6), 975−979.
(8) Hoffmann, R. D.; Pottgen, R.; Rosenhahn, C.; Mosel, B. D.; Kunnen, B.; Kotzyba, G. *J. Solid State Chem.* **1999**, *145* (1), 283−290.
(9) Hoffmann, R. D.; Pottgen, R.; Zaremba, V. I.; Kalychak, Y. M. *Z. Naturforsch., B: Chem. Sci.* **2000**, *55* (9), 834−840.
(10) Morris, G. D.; Heffner, R. H.; Moreno, N. O.; Pagliuso, P. G.; Sarrao, J. L.; Dunsiger, S. R.; Nieuwenhuys, G. J.; MacLaughlin, D. E.; Bernal, O. O. *Phys. Rev. B: Condens. Matter Mater. Phys.* **2004**, *69*, (21).
(11) Macaluso, R. T.; Sarrao, J. L.; Moreno, N. O.; Pagliuso, P. G.; Thompson, J. D.; Fronczek, F. R.; Hundley, M. F.; Malinowski, A.; Chan, J. Y. *Chem. Mater.* **2003**, *15* (6), 1394−1398.
(12) Zaremba, R. I.; Kalychak, Y. M.; Rodewald, U. C.; Pottgen, R.; Zaremba, V. I. *Z. Naturforsch., B: Chem. Sci.* **2006**, *61* (8), 942−948.
(13) Zaremba, V. I.; Dubenskiy, V. P.; Rodewald, U. C.; Heying, B.; Pottgen, R. *J. Solid State Chem.* **2006**, *179* (3), 891−897.
(14) Lukachuk, M.; Kalychak, Y. M.; Dzevenko, M.; Pottgen, R. *J. Solid State Chem.* **2005**, *178* (4), 1247−1253.
(15) Wendorff, M.; Rohr, C. *Z. Anorg. Allg. Chem.* **2005**, *631* (2−3), 338−349.
(16) Lukachuk, M.; Hoffmann, R. D.; Pottgen, R. *Monatsh. Chem.* **2005**, *136* (2), 127−135.
(17) Wendorff, M.; Rohr, C. *Z. Naturforsch., B: Chem. Sci.* **2004**, *59* (6), 619−628.
(18) Hlukhyy, V.; Zaremba, V. I.; Kalychak, Y. M.; Pottgen, R. *J. Solid State Chem.* **2004**, *177* (4−5), 1359−1364.

10.1021/ic700633b CCC: $37.00 © 2007 American Chemical Society
Published on Web 07/27/2007

In a recent review, we highlighted the considerable opportunities for materials exploration that exist in molten metals as fluxes.[25] We have begun to investigate the use of In as a flux for the exploratory synthesis of intermetallic compounds.[26,27] Prior work with In as a flux focused mainly on the crystal growth of known phases.[28−30] Considerably less work has been reported on the use of molten indium as a medium for the exploratory synthesis of intermetallic compounds, but interest in this approach has been growing.[28,31−34,35−37] Given the success of liquid aluminum and gallium as solvents for the stabilization of complex intermetallics, it is reasonable to expect that indium may also be a productive solvent.[38−46] Generally, reactivity patterns in liquid metal fluxes are not well-developed.

Previously, we demonstrated that reactions carried out in excess indium can produce compounds that do not form by direct combination of the elements. Specifically, we showed that it was possible to produce a new form of $RENiGe_2$ (β form) that crystallizes in the $YIrGe_2$ structure instead of the $CeNiSi_2$ structure, which is the thermodynamically stable form and can be produced by direct combination reactions.[27] Reactions of RE, TM, and Ge in liquid In have a lower tendency to form quaternary phases of the type RE/TM/In/Ge than do reactions in liquid Al and Ga.[38,45] Instead, many reactions carried out in excess In generally result in crystals of known phases including $RENi_2Ge_2$, RENiGe, and $RENi_5Ge_3$. Recently, however, in one case we succeeded in synthesizing $RE_4Ni_2InGe_4$ (RE = Dy, Ho, Er, Tm).[26] Because of the general tendency of Ge to be included in the structure with the exclusion of In resulting in TM/Ge networks, we decided to pursue a course where Ge was left out of the reaction so that we could more easily study the structural chemistry of RE/TM/In networks.

Here, we present $REAu_2In_4$ (RE = La, Ce, Pr, Nd), the most indium-rich phases yet reported for this combination of elements. The syntheses, crystal structure, thermal stability, and magnetic properties of these compounds are described. Electronic structure calculations using density functional theory (DFT) for the La analogue are also reported. They provide useful insight into the nature of bonding in these compounds and the role of Au d electrons in the electronic density of states (DOS) near the Fermi energy. The analogous $YbAu_2In_4$ has a different monoclinic structure ($P2_1/m$) and will be reported separately.

Experimental Section

Reagents. The following reagents were used without further purification: La metal (~40 mesh powder, 99.9%, Cerac, Milwaukee, WI), Ce metal (~250 mesh powder, 99.9%, Research Chemicals, Phoenix, AZ), Pr metal (~ 250 mesh, 99.9%, Research Chemicals, Phoenix, AZ), Nd metal (~250 mesh powder, 99.9%, Research Chemicals, Phoenix, AZ), Au metal (ingot, 99.9%, Research Chemicals, Phoenix, AZ), and In (3−5 mm teardrops, 99.99%, Cerac, Milwaukee, WI).

Synthesis. Method A. $REAu_2In_4$ (RE = La, Ce, Pr, Nd) were produced by combining 0.5 mmol of the rare-earth metal, 1 mmol of Au, and 8 of mmol In in an Al_2O_3 crucible, then flame-sealing them under a reduced atmosphere of 10^{-4} mbar in a fused silica tube. The reactants were heated to 1000 °C over the course of 10 h, held at 1000 °C for 72 h, then cooled to 150 °C over 24 h. Initial isolation of the product from the flux was done by decanting the excess indium from the crucible. Because indium tended to wet the surface of the crystals, etching with glacial acetic acid was required. The acetic acid etch did not significantly affect the products even after several days of being submerged. The yields were generally 70% based on the initial rare-earth mass, with a purity of 70 to 80%. The main impurities were cubic $AuIn_4$ and $REIn_3$, which can be etched away by acetic acid over the course of a week.

(19) Galadzhun, Y. V.; Zaremba, V. I.; Kalychak, Y. M.; Davydov, V. M.; Pikul, A. P.; Stepien-Damm, A.; Kaczorowski, D. *J. Solid State Chem.* **2004**, *177* (1), 17−25.
(20) Zaremba, V. I.; Rodewald, U. C.; Hoffmann, R. D.; Kalychak, Y. M.; Pottgen, R. *Z. Anorg. Allg. Chem.* **2003**, *629* (7−8), 1157−1161.
(21) Bailey, M. S.; McGuire, M. A.; DiSalvo, F. J. *J. Solid State Chem.* **2005**, *178* (11), 3494−3499.
(22) ShreeveKeyer, J. L.; Haushalter, R. C.; Lee, Y. S.; Li, S. C.; O'Connor, C. J.; Seo, D. K.; Whangbo, M. H. *J. Solid State Chem.* **1997**, *130* (2), 234−249.
(23) Zaremba, V. I.; Dubenskiy, V. P.; Kalychak, Y. A.; Hoffmann, R. D.; Pottgen, R. *Solid State Sci.* **2002**, *4* (10), 1293−1298.
(24) Li, B.; Corbett, J. D. *J. Am. Chem. Soc.* **2006**, *128* (38), 12392−12393.
(25) Kanatzidis, M. G.; Pottgen, R.; Jeitschko, W. *Angew. Chem., Int. Ed.* **2005**, *44* (43), 6996−7023.
(26) Salvador, J. R.; Kanatzidis, M. G. *Inorg. Chem.* **2006**, *45* (18), 7091−7099.
(27) Salvador, J. R.; Gour, J. R.; Bilc, D.; Mahanti, S. D.; Kanatzidis, M. G. *Inorg. Chem.* **2004**, *43* (4), 1403−1410.
(28) Canfield, P. C.; Fisk, Z. *Philos. Mag. B* **1992**, *65* (6), 1117−1123.
(29) Bud'ko, S. L.; Islam, Z.; Wiener, T. A.; Fisher, I. R.; Lacerda, A. H.; Canfield, P. C. *J. Magn. Magn. Mater.* **1999**, *205* (1), 53−78.
(30) Fisher, I. R.; Islam, Z.; Canfield, P. C. *J. Magn. Magn. Mater.* **1999**, *202* (1), 1−10.
(31) Zaremba, V. I.; Kalychak, Y. M.; Tyvanchuk, Y. B.; Hoffmann, R. D.; Moller, M. H.; Pottgen, R. *Z. Naturforsch., B: Chem. Sci.* **2002**, *57* (7), 791−797.
(32) Pagliuso, P. G.; Thompson, J. D.; Sarrao, J. L.; Sercheli, M. S.; Rettori, C.; Martins, G. B.; Fisk, Z.; Oseroff, S. B. *Phys. Rev. B: Condens. Matter Mater. Phys.* **2001**, *6314* (14).
(33) Pagliuso, P. G.; Sarrao, J. L.; Thompson, J. D.; Hundley, M. F.; Sercheli, M. S.; Urbano, R. R.; Rettori, C.; Fisk, Z.; Oseroff, S. B. *Phys. Rev. B: Condens. Matter Mater. Phys.* **2001**, *6309* (9).
(34) Macaluso, R. T.; Sarrao, J. L.; Pagliuso, P. G.; Moreno, N. O.; Goodrich, R. G.; Browne, D. A.; Fronczek, F. R.; Chan, J. Y. *J. Solid State Chem.* **2002**, *166* (1), 245−250.
(35) Bobev, S.; Fritsch, V. *Acta Crystallogr., Sect. E: Struct. Rep. Online* **2006**, *62*, I182−I183.
(36) Tobash, P. H.; Lins, D.; Bobev, S.; Lima, A.; Hundley, M. F.; Thompson, J. D.; Sarrao, J. L. *Chem. Mater.* **2005**, *17* (22), 5567−5573.
(37) Jiang, J.; Payne, A. C.; Olmstead, M. M.; Lee, H. O.; Klavins, P.; Fisk, Z.; Kauzlarich, S. M.; Hermann, R. P.; Grandjean, F.; Long, G. J. *Inorg. Chem.* **2005**, *44* (7), 2189−2197.
(38) Sieve, B.; Chen, X. Z.; Henning, R.; Brazis, P.; Kannewurf, C. R.; Cowen, J. A.; Schultz, A. J.; Kanatzidis, M. G. *J. Am. Chem. Soc.* **2001**, *123* (29), 7040−7047.
(39) Chen, X. Z.; Sieve, B.; Henning, R.; Schultz, A. J.; Brazis, P.; Kannewurf, C. R.; Cowen, J. A.; Crosby, R.; Kanatzidis, M. G. *Angew. Chem., Int. Ed.* **1999**, *38* (5), 693−696.
(40) Chen, X. Z.; Sportouch, S.; Sieve, B.; Brazis, P.; Kannewurf, C. R.; Cowen, J. A.; Patschke, R.; Kanatzidis, M. G. *Chem. Mater.* **1998**, *10* (10), 3202−3211.
(41) Wu, X. U.; Latturner, S.; Kanatzidis, M. G. *Inorg. Chem.* **2006**, *45* (14), 5358−5366.
(42) Latturner, S. E.; Bilc, D.; Mahanti, S. D.; Kanatzidis, M. G. *Inorg. Chem.* **2003**, *42* (24), 7959−7966.
(43) Latturner, S. E.; Kanatzidis, M. G. *Chem. Commun.* **2003**, (18), 2340−2341.
(44) Zhuravleva, M. A.; Bilc, D.; Pcionek, R. J.; Mahanti, S. D.; Kanatzidis, M. G. *Inorg. Chem.* **2005**, *44* (7), 2177−2188.
(45) Zhuravleva, M. A.; Pcionek, R. J.; Wang, X. P.; Schultz, A. J.; Kanatzidis, M. G. *Inorg. Chem.* **2003**, *42* (20), 6412−6424.
(46) Zhuravleva, M. A.; Kanatzidis, M. G. *Z. Naturforsch., B: Chem. Sci.* **2003**, *58* (7), 649−657.

Table 1. Crystallographic Data for $REAu_2In_4$ (RE = La, Ce, Pr, Nd)

empirical formula	$LaAu_2In_4$	$CeAu_2In_4$	$PrAu_2In_4$	$NdAu_2In_4$
fw	992.13	993.33	994.13	997.46
cryst syst	orthorhombic	orthorhombic	orthorhombic	orthorhombic
space group	*Pnma*	*Pnma*	*Pnma*	*Pnma*
a (Å)	18.506(2)	18.514(3)	18.420(4)	18.406(2)
b (Å)	4.6865(6)	4.6624(8)	4.6202(9)	4.6114(5)
c (Å)	7.3414(9)	7.389(1)	7.376(2)	7.4073(7)
V (Å^3)	636.7(1)	637.8(2)	627.7(2)	628.7(1)
Z	4	4	4	4
D (calcd) (g/cm^3)	10.350	10.345	10.519	10.538
abs coeff μ (mm^{-1})	66.554	66.869	68.452	68.852
T (K)	293	293	293	293
reflns collected/unique/R(int)	5596/813/ 0.0427	6701/1037/0.0681	5183/819/0.0287	2212/536/0.0285
data/restraints/params	813/0/44	1037/0/44	819/0/44	536/0/44
GOF on F^2	1.195	1.084	1.128	1.214
R indices (all data) (R1/wR2)[a]	0.0349/0.0859	0.0430/0.0968	0.0382/0.0778	0.0249/0.0587

[a] $R1 = \sum||F_o| - |F_c||/\sum|F_o|$ and $wR2 = [\sum(|F_o^2 - F_c^2|)^2/\sum(wF_o^2)^2\ ]^{1/2}$.

Method B. $REAu_2In_4$ were also prepared by combining the reactants in their stoichiometric ratios in an Al_2O_3 crucible, then flame-sealing the reactants under a reduced atmosphere of 10^{-4} mbar in a fused silica tube. The reactants were then heated to 1000 °C over 10 h and held there for an additional 120 h before cooling to room temperature over the course of 48 h. The target phase was obtained in a pure form (as judged by powder X-ray diffraction) in nearly quantitative yields, though crystal size and quality were inferior to those obtained by method A.

X-ray Crystallography. Single-crystal X-ray diffraction data were collected at room temperature on crystals produced from excess In using a Bruker AXS SMART CCD diffractometer with graphite-monochromatized Mo Kα ($\lambda = 0.71073$ Å) radiation. Unit-cell refinement and data merging were done with the *SAINT* program, and an empirical absorption correction was applied using the program *SADABS*.[47] The originally determined unit cell of $LaAu_2In_4$ led to the assignments of $a = 4.6865(6)$ Å, $b = 7.3414(9)$ Å, and $c = 18.506(2)$ Å. Inspection of the systematic absences found the cell to be primitive with the unambiguous determination of the space group *Pcmn*. A structural solution in *Pcmn* was obtained for $LaAu_2In_4$ by direct methods using the program *SHELXS*,[48] and the final structural refinement was completed with the *SHELXTL* suite of programs.[49] The space group *Pcmn* is a nonstandard representation of the space group *Pnma*; the appropriate transformation matrix was applied. The structure was then refined using the standard setting. Solutions of the Ce, Pr, and Nd analogues were obtained by using the solution of $LaAu_2In_4$ as a starting point, with the final refinement done using *SHELXTL*. Data collection and refinement details for all compounds are given in Table 1. Atomic coordinates and isotropic displacement parameters for $LaAu_2In_4$, $CeAu_2In_4$, $PrAu_2In_4$, and $NdAu_2In_4$ can be found in Table 2.

Phase identity and purity was confirmed by powder X-ray diffraction carried out on an Inel diffractometer with Cu Kα radiation. The experimental powder patterns were compared with the calculated powder patterns generated from the single-crystal structural refinements. Powder patterns were calculated using the *CERIUS2* software package.[50]

Table 2. Atomic Coordinates ($\times 10^4$) and Equivalent Isotropic Displacement Parameters (Å$^2 \times 10^3$) for $REAu_2In_4$ (RE = La, Ce, Pr, Nd)

atom	Wyckoff position	x	y	z	U(eq)[a]
Au(1)	4c	2820(1)	2500	5291(1)	12(1)
Au(2)	4c	376(1)	2500	2417(1)	13(1)
La	4c	1406(1)	7500	5174(1)	12(1)
In(1)	4c	4316(1)	2500	4894(2)	15(1)
In(2)	4c	349(1)	2500	3481(2)	13(1)
In(3)	4c	1892(1)	2500	2283(2)	10(1)
In(4)	4c	1841(1)	2500	8215(2)	11(1)
Au(1)	4c	2825(1)	2500	5314(1)	12(1)
Au(2)	4c	379(1)	2500	2433(1)	12(1)
Ce	4c	1411(1)	7500	5208(1)	11(1)
In(1)	4c	4324(1)	2500	4875(2)	14(1)
In(2)	4c	348(1)	2500	3536(2)	12(1)
In(3)	4c	1888(1)	2500	2318(2)	10(1)
In(4)	4c	1844(1)	2500	8234(2)	11(1)
Au(1)	4c	2820(1)	2500	5340(1)	12(1)
Au(2)	4c	383(1)	2500	2417(1)	13(1)
Pr	4c	1406(1)	7500	5174(1)	12(1)
In(1)	4c	4316(1)	2500	4894(2)	15(1)
In(2)	4c	349(1)	2500	3481(2)	13(1)
In(3)	4c	1892(1)	2500	2283(2)	10(1)
In(4)	4c	1841(1)	2500	8215(2)	11(1)
Au(1)	4c	2819(1)	2500	5351(1)	9(1)
Au(2)	4c	383(1)	2500	2443(1)	9(1)
Nd	4c	1420(1)	7500	5251(1)	9(1)
In(1)	4c	4329(1)	2500	4864(1)	10(1)
In(2)	4c	350(1)	2500	3587(1)	9(1)
In(3)	4c	1884(1)	2500	2364(1)	7(1)
In(4)	4c	1848(1)	2500	3268(1)	8(1)

[a] U(eq) is defined as one-third of the trace of the orthogonalized U_{ij} tensor.

Elemental Analysis. Semiquantitative microprobe elemental analysis was performed on several single crystals of each of the analogues, including the crystals used for single-crystal X-ray diffraction experiments. The spectra were collected on a JEOL JSM-35C scanning electron microscope equipped with a Tracor Noran energy-dispersive spectrometer with a Norvar window capable of standardless quantitation of elements with $Z \geq 4$. Spectra were collected with an accelerating voltage of 25 kV and 60 s acquisition time. The spectra contained the L and M lines of La, Au, and In and a peak attributed to the K line of C. No other elements were detected. Spectral contamination by carbon is likely from the tape on which the samples were mounted. Standardless quantitation of the spectra led to the following atomic ratios: 1.00 (±0.03), 2.25 (±0.08), and 3.6 (±0.1) for La, Au, and In, respectively. These values are in reasonably good agreement with the stoichiometric

(47) *SAINT*, version 4; Siemens Analytical X-ray Instruments, Inc.: Madison, WI. Sheldrick, G. M. *SADABS*; University of Göttingen: Göttingen, Germany.
(48) *SHELXS-97*; Bruker Analytical X-ray Instruments, Inc.: Madison, WI, 1990.
(49) Sheldrick, G. M. *SHELXTL. Structure Determination Program*, version 5.0; Siemens Analytical X-ray Instruments, Inc.: Madison, WI, 1995.
(50) *CERIUS2*, version 1.6; Molecular Simulations, Inc.: Cambridge, U.K., 1994.

ratios obtained from the crystallographic refinement, within the limitation of the technique. Similar stoichiometric ratios were determined for the other RE analogues as well.

Differential Thermal Analysis. Differential thermal analysis (DTA) was carried out with a Shimadzu DTA-50 instrument against an alumina standard. The samples were hand-selected crystals placed in a carbon-coated fused silica ampule, which was flame-sealed under a reduced atmosphere of 10^{-4} mbar. The samples were heated at a rate of 10 °C per minute up to 1000 °C, and then cooled to 150 °C at the same rate. The cycle was repeated up to 1000 °C with the same heating and cooling rates. The DTA data for the product of the direct combination and flux reaction are available in the Supporting Information.

Electronic Structure Calculations. Ab initio electronic structure calculations were performed on $LaAu_2In_4$ using the self-consistent all-electron full-potential linearized augmented plane-wave (FP-LAPW)[51] method within the DFT formalism incorporated in WIEN2k[52] with a generalized gradient approximation (GGA) of the Perdew−Burke−Ernzerhof's type[53,54] for the exchange and correlation potentials. These calculations were carried out only for the La system because of the inability of GGA to properly take into account the strong Coulomb correlation effects associated with partially filled f levels (as in the other rare-earth compounds). Since La^{3+} is formally an f^0 ion, this difficulty is avoided. Self-consistent iterations were performed with 56 *k* points in the reduced Brillouin zone (BZ) with a cutoff between the valence and core states of −6.0 Ry; convergence was assumed when the total energy difference between cycles was within 0.0001 Ry. Since FP-LAPW calculations are computationally very demanding, it is not easy to carry out detailed relaxation studies using this method. We have, therefore, used the *Vienna Ab Initio Simulation Package* (VASP)[55,56] and the projector augmented wave (PAW)[57,58] method to carry out such calculations. In the latter, we used 70 *k* points in the reduced BZ for ionic relaxation, 162 *k* points for charge density, energy and, electron localization function (ELF)[59,60] calculations, and 264 *k* points to produce high quality DOS. Scalar relativistic effects were included in both LAPW and PAW calculations. Spin−orbit interaction (SOI) was included in some calculations to see whether it significantly altered the electronic structure, particularly near the Fermi energy. Convergence was assumed when the total energy difference between two cycles was 0.0001 eV.

Magnetic Measurements. Magnetic measurements were carried out on a Quantum Design MPMS SQUID magnetometer. Measurements were performed on handpicked single crystals, which were placed in an envelope made of Kapton tape. Temperature-dependent susceptibility data was collected in both field-cooled and zero-field-cooled modes with an applied field of 1000 Oe for $LaAu_2In_4$, 500 Oe for the Ce analogue, and 2000 Oe for $PrAu_2In_4$ and $NdAu_2In_4$. Magnetization data were also collected at 2 K for all compounds with fields sweeping from −55 to 55 kOe. It is important to make a diamagnetic core correction to obtain a value of the magnetic susceptibility associated with the conduction (valence) electrons. In intermetallic compounds containing Au, the Au d bands lie below the Fermi level, and we assumed that the Au d electrons can be treated as core; although in some intermetallics, it is believed that Au behaves like a Au^{1-};[61] i.e., two valence electrons are bound to Au. Since we do not know the precise electronic structure associated with these two extra valence electrons, we considered them as a part of the conduction band. Thus, for the core diamagnetic corrections, we used the configurations La^{3+}, Au^{+}, and In^{3+}. We used values of -2.0×10^{-5} emu/mol for La^{3+},[62] -4.0×10^{-5}-emu/mol for Au^{+},[63−66] and -1.9×10^{-5}emu/mol for In^{3+}.[62] Thus, for $LaAu_2In_4$, the core diamagnetic contribution was determined to be -17.6×10^{-5} emu/mol La.

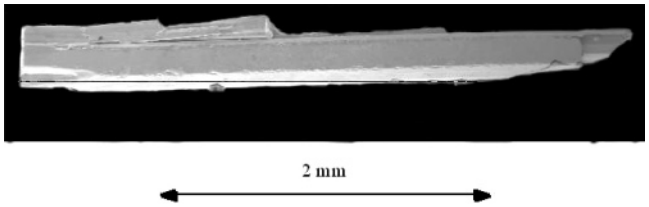

Figure 1. Scanning electron micrograph of a indium flux-grown $LaAu_2In_4$ crystal, which shows the length of the rod is in excess of 3.0 mm.

Results and Discussion

Reaction Chemistry. The La, Ce, Nd, and Pr analogues of $REAu_2In_4$ were formed either by providing excess molten In as a flux or by heating a stoichiometric combination of the elements. Crystals of $REAu_2In_4$ grown from In flux using an isotherm of 1000 °C for 72 h were relatively large (several millimeters in length). $REAu_2In_4$ crystals could either crystallize from indium solution during the cooling step or they could form during the isotherm step. Figure 1 shows a scanning electron micrograph of a $LaAu_2In_4$ crystal grown from liquid In.

The products of the direct combination reactions formed as ingots that did not wet the walls of the Al_2O_3 crucible. The surface of the ingot was dull, likely due to the presence of a small amount of an unknown oxide. We observed that if the direct combination reaction was stopped after 72 h, the target phase was contaminated with $AuIn_4$, $REIn_3$, and other unidentified phases. When the isotherm was extended to 5 days, the target phase could be obtained in a nearly pure form (estimated to be between 90 and 95%). Reflections attributable to $REIn_3$ were still observed in the powder

(51) D. J. Singh.
(52) Blaha, P.; K. S.; Madsen, G. K. H.; Kvasnicka, D.; Luitz, J. *WIEN2k, An Augmented Plane Wave + Local Orbitals Program for Calculating Crystal Properties*; Schwarz, K., Ed.; Technische Universitat Wien: Austria, 2001.
(53) Perdew, J. P.; Burke, K.; Ernzerhof, M. *Phys. Rev. Lett.* **1997**, *78* (7), 1396−1396.
(54) Perdew, J. P.; Burke, K.; Ernzerhof, M. *Phys. Rev. Lett.* **1996**, *77* (18), 3865−3868.
(55) Kresse, G.; Hafner, J. *Phys. Rev. B: Condens. Matter Mater. Phys.* **1994**, *49* (20), 14251−14269.
(56) Kresse, G.; Hafner, J. *Phys. Rev. B*: *Condens. Matter Mater. Phys.* **1993**, *47* (1), 558−561.
(57) Blochl, P. E. *Phys. Rev. B*: *Condens. Matter Mater. Phys.* **1994**, *50* (24), 17953−17979.
(58) Kresse, G.; Joubert, D. *Phys. Rev. B*: *Condens. Matter Mater. Phys.* **1999**, *59* (3), 1758−1775.
(59) Savin, A.; Jepsen, O.; Flad, J.; Andersen, O. K.; Preuss, H.; Vonschnering, H. G. *Angew. Chem., Int. Ed. Engl.* **1992**, *31* (2), 187−188.
(60) Kresse, G.; Furthmuller, J. *Phys. Rev. B*: *Condens. Matter Mater. Phys.* **1996**, *54* (16), 11169−11186.
(61) Feldmann, C.; Jansen, M. *Z. Anorg. Allg. Chem.* **1995**, *621* (2), 201−206.
(62) Selwood, P. W. *Magnetochemistry*, 2nd ed.; Interscience Publishers: New York, 1956; pp 70−78.
(63) Vajenine, G. V.; Hoffmann, R. *J. Am. Chem. Soc.* **1998**, *120* (17), 4200−4208.
(64) Latturner, S. E.; Bilc, D.; Mahanti, S. D.; Kanatzidis, M. G. *Chem. Mater.* **2002**, *14* (4), 1695−1705.
(65) Niemann, S.; Jeitschko, W. *J. Alloys Compd.* **1995**, *221*, 235−239.
(66) Niemann, S.; Jeitschko, W. *J. Solid State Chem.* **1995**, *116* (1), 131−135.

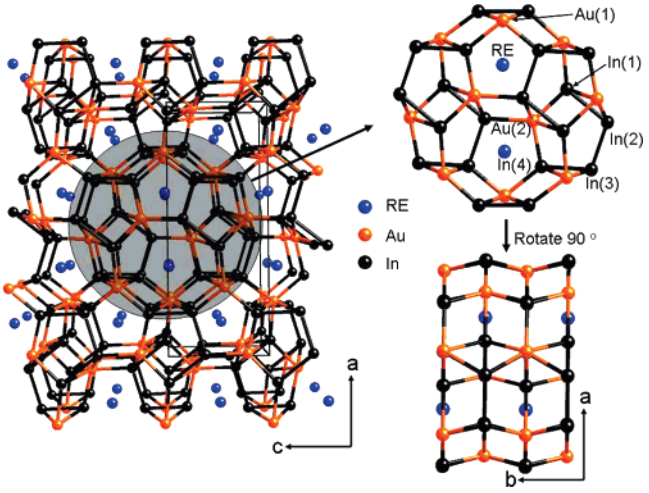

Figure 2. Overall structure of $REAu_2In_4$ as viewed along the *b* axis. The shaded portion in the structure is expanded to show the central polyhedral cluster that propagates along the *b* axis. The central cluster unit, when rotated 90°, shows the connectivity along the *b* axis.

patterns, though their intensities were very low. This result implies that the reaction rate for the formation of $REAu_2In_4$, is much slower in the direct combination reaction compared with the In flux reaction. This is likely because the product melts well above the reaction temperature (confirmed with DTA), and the kinetics of formation are diffusion limited. In liquid indium, the diffusion rate for reactants is rapid yielding the target phase more quickly. The In flux provides conditions resembling those found in conventional solution chemistry that lead to faster reaction rates.

Structure. All members of $REAu_2In_4$ (RE = La, Ce, Pr, Nd) are isostructural, composed of a complex $[Au_2In_4]^{3-}$ polyanion network in which the RE ions are embedded. Figure 2 shows the overall structure of the title compounds as viewed along the *b* axis. The highlighted portion of the structure is expanded to show the principal building unit of the compound. The structure is composed of four crystallographically distinct In atoms, two Au atoms, and one unique RE atom. Rotating the highlighted portion of the structure by 90° gives the alternative view along the *c* axis, also seen in Figure 2. The $[Au_2In_4]^{3-}$ network is a three-dimensional entity composed of the In tetramer units shown in Figure 3A. The lengths of the In−In bonds range from 2.987(2) Å for In(2)−In(3) and In(3)−In(4) to 3.129(2) Å for In(1)−In(2) in $LaAu_2In_4$ and from 2.966(2) Å for In(2)−In(3) to 3.172(1) Å for In(1)−In(2) in $NdAu_2In_4$. This tetrameric In segment is the defining characteristic of the polyindide nature of the compounds.

The gold atoms are isolated from one another, forming bonds only with In and RE for the reasons discussed below. Each of the Au atoms forms seven bonds to the surrounding In atoms, with distances ranging from 2.784(1) to 2.8651(8) Å for Au(1) in $LaAu_2In_4$, from 2.7996(6) to 2.805(1) Å for Au(1) in $NdAu_2In_4$, from 2.773(1) to 3.0202(9) Å for Au(2) in $LaAu_2In_4$, and from 2.7636(1) to 2.969(1) Å for Au(2) in $NdAu_2In_4$. In addition, each Au atom forms two bonds with the RE atoms defining a nine-coordinate site.

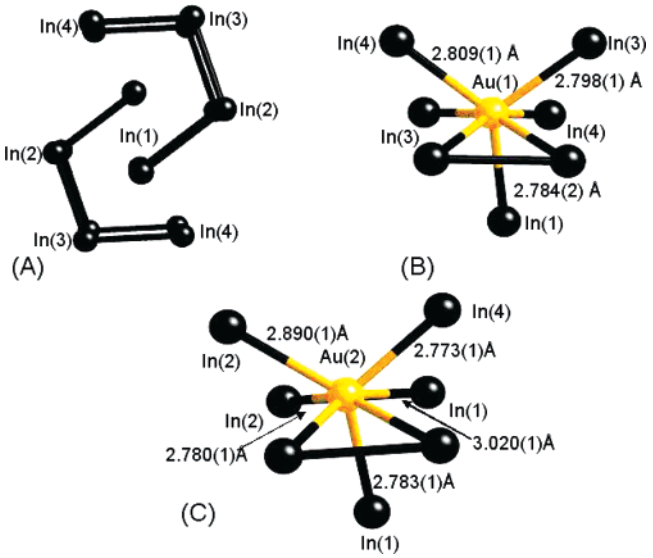

Figure 3. (A) Depiction of the interweaving In tetramers. Au and RE atoms were removed to emphasize this structural unit. (B) The coordination sphere of Au(1) out to 3.3 Å; bond distances listed are for $LaAu_2In_4$. (C) The coordination sphere of Au(2) out to 3.3 Å; bond distances listed are for $LaAu_2In_4$.

Table 3. Bond Distances (Å) for $REAu_2In_4$ (RE = La, Ce, Pr, Nd)

	RE = La	RE = Ce	RE = Pr	RE = Nd
Au(1)−In(1)	2.784(1)	2.800(1)	2.796(1)	2.803(1)
Au(1)−In(3)	2.798(1)	2.809(1)	2.797(1)	2.7996(6)
Au(1)−In(4)	2.809(1)	2.817(1)	2.802(1)	2.805(1)
Au(1)−In(3) × 2	2.8129(8)	2.8135(8)	2.7980(8)	2.804(1)
Au(1)−In(4) × 2	2.8651(8)	2.8602(8)	2.8389(8)	2.805(1)
Au(1)−RE × 2	3.5138(9)	3.5013(9)	3.4670(9)	3.4583(7)
Au(2)−In(4)	2.773(1)	2.775(1)	2.766(1)	2.7636(1)
Au(2)−In(2) × 2	2.7798(8)	2.7856(8)	2.7756(8)	2.7780(6)
Au(2)−In(1)	2.783(1)	2.787(1)	2.779(1)	2.782(1)
Au(2)−In(2)	2.890(1)	2.880(1)	2.857(1)	2.857(1)
Au(2)−In(1) × 2	3.0202(9)	2.9985(9)	2.9740(9)	2.9689(7)
Au(2)−RE × 2	3.4397(9)	3.4338(9)	3.4059(8)	3.4044(6)
Au(2)−RE	3.807(1)	3.847(1)	3.876(1)	3.891(1)
RE−In(3) × 2	3.287(1)	3.282(1)	3.259(1)	3.2590(8)
RE−In(2) × 2	3.295(1)	3.292(1)	3.275(1)	3.2731(8)
RE−In(4) × 2	3.335(1)	3.327(1)	3.308(1)	3.3061(8)
RE−In(2)	3.394(2)	3.387(1)	3.371(1)	3.368(1)
RE−In(3)	3.510(1)	3.513(1)	3.493(1)	3.493(1)
In(1)−In(2)	3.129(2)	3.153(2)	3.159(2)	3.172(1)
In(2)−In(3)	2.987(2)	2.990(2)	2.969(2)	2.966(1)
In(3)−In(4)	2.988(2)	3.019(2)	3.016(2)	3.035(1)

The bonding geometries for the two crystallographically unique Au sites are identical; they differ only by which In atoms they bind and at what distances. The coordination environment for Au(1) and Au(2) is shown in Figures 3B and 3C, respectively (RE atoms were omitted for clarity).

The Au−In distances mentioned above and listed in Table 3 agree well with other reported Au−In distances of related compounds and are consistent with strong metallic In−In and Au−In bonding.[7−9,20] The Au atoms bond with In to form Au_2In_2 parallelograms, a common structural motif of the RE/Au/In structures such as $RE_2Au_3In_5$[5] and $La_3Au_4In_7$.[6] There is a large structural diversity observed in systems containing these Au_2In_2 units, and it is due to the variety of ways in which this unit can pack and condense to form extended structures.

The RE atom is in a cage coordination, forming bonds with eight In atoms and four Au atoms as shown in Figure

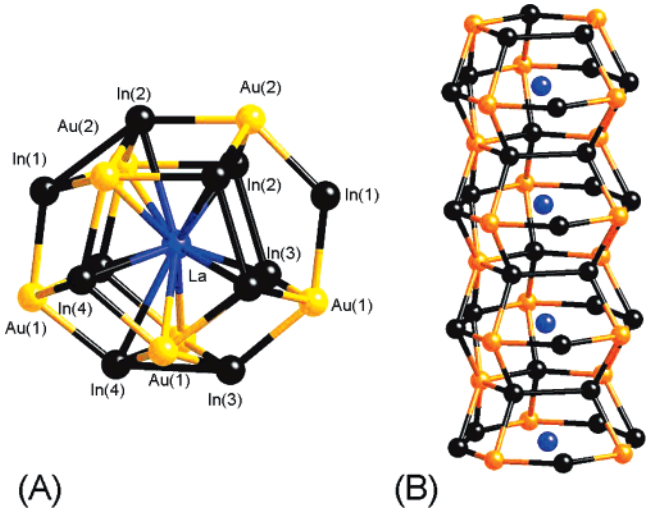

Figure 4. (A) Coordination environment of the RE atoms at the center of the pentagonal and octagonal channels. The RE atom is coordinated by eight In atoms and four Au atoms. (B) Illustration shows the La atoms residing in the center of the pentagonal and octagonal channels and highlights the connectivity of the alternating five- and eight-member rings.

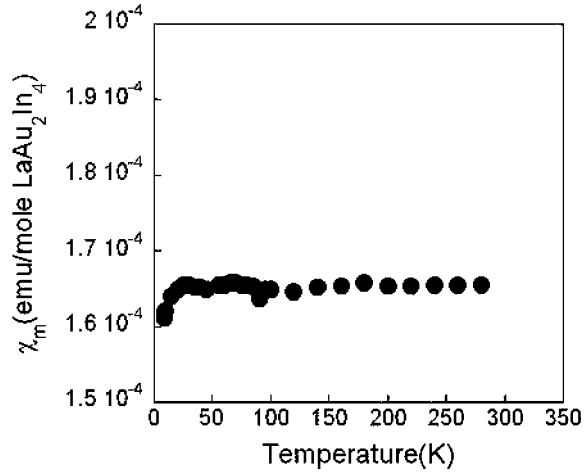

Figure 5. Magnetic susceptibility for $LaAu_2In_4$ collected with an applied field of 1 kOe with zero-field cooling.

4A. By inspection of the immediate coordination environment in Figure 4A it is evident that these cages are fused through "Au_2In_3" pentagons and "Au_3In_5" octagons, which stack alternately along the *b* axis. The RE atoms reside in the center of a pentagonal/octagonal channel that runs parallel to the *b* axis, as shown explicitly in Figure 4B. The closest RE separations are crystallographically imposed and are equal to the *b*-axis lattice parameter for each of the compounds (ranging from 4.6865(6) Å for $LaAu_2In_4$ to 4.6114(5) Å for $NdAu_2In_4$). The adjacent channels composed of alternating pentagonal and octagonal rings interpenetrate to form the core building unit seen in Figure 2.

Magnetic Measurements. $LaAu_2In_4$. Temperature-dependent susceptibility measurements performed on $LaAu_2In_4$ indicated temperature-independent paramagnetism (TIP) from 20 to 300 K. The mean value of the susceptibility after correcting for the container and core correction (-17.6×10^{-5}) was found to be 1.66×10^{-4} emu/mol La (Figure 5). The TIP response in the higher temperature region indicates that the La has a f^0 electronic configuration and is in the 3+ oxidation state, and also, the Au atoms are diamagnetic (d^{10}), as is often the case in polar intermetallics.[43,63,64] Other metallic systems have both comparable and larger paramagnetic susceptibilities. For example, $Y_{0.67}Ni_2Ga_{5-x}Ge_x$ has a susceptibility of $+1.3 \times 10^{-4}$ emu/mol Y[67] and $La_{5-x}Ni_{12}Sn_{24}$ has a susceptibility of $+2.83 \times 10^{-3}$ emu/mol La.[68,69]

$CeAu_2In_4$. The magnetic susceptibility data for $CeAu_2In_4$ can be seen in Figure 6A. The data follow the Curie−Weiss law from 300 to 2 K with no indication that the compound magnetically orders. The effective magnetic moment obtained from the inverse susceptibility versus temperature function was 2.44 μ_B, which is in reasonably good agreement with the calculated value for a Ce^{3+} ion, which is 2.54 μ_B. The Weiss constant is small and negative ($\theta = -2.5$ K), indicating weak antiferromagnetic interactions among the Ce^{3+} ions. We see from the resulting effective magnetic moment that Ce^{3+} is the only species responsible for the magnetic susceptibility, with all other atoms contributing a small amount of temperature-independent Pauli susceptibility (as in the La compound).

The magnetization data at 2 K for $CeAu_2In_4$ can be found in Figure 6B. There is a linear response in the magnetization curve up to a field of 22 kOe, at which point the slope continuously changes until approximately 30 kOe, when it again becomes linear, but with a much shallower slope. The response remains linear up to 55 kOe. The material does not appear to saturate, as the magnetization still has a strong dependence on the applied field up to the highest attainable field. Also, the moment reaches a value of only 1.0 μ_B at 55 kOe. This value is about half that predicted for a Ce^{3+} ion.

$PrAu_2In_4$. Figure 6C shows the magnetic susceptibility data for $PrAu_2In_4$. This compound obeys Curie−Weiss law over the entire temperature range investigated with a resulting effective magnetic moment of 3.87 μ_B. A very small Weiss constant θ of −0.28 K was obtained from the data, but is negligibly small. The effective magnetic moment obtained from the susceptibility measurements is in good agreement with the theoretical value for a Pr^{3+} ion, 3.7 μ_B. The extremely small Weiss constant indicates practically no magnetic interaction between the Pr^{3+} ions. As was the case with $CeAu_2In_4$, the Pr^{3+} ion is the only paramagnetic species in the compound.

The magnetization curve for $PrAu_2In_4$ at 2 K can be found in Figure 6D. The moment increases linearly with an applied field up to about 15 kOe, at which point the field dependence becomes weaker and the moment begins to saturate. The field dependence again becomes linear, though with a shallower slope similar to the behavior observed for $CeAu_2In_4$. This

(67) Zhuravleva, M. A.; Chen, X. Z.; Wang, X. P.; Schultz, A. J.; Ireland, J.; Kannewurf, C. K.; Kanatzidis, M. G. *Chem. Mater.* **2002**, *14* (7), 3066−3081.
(68) Zhuravleva, M. A.; Bilc, D.; Mahanti, S. D.; Kanatzidis, M. G. *Z. Anorg. Allg. Chem.* **2003**, *629* (2), 327−334.
(69) Although a direct numerical comparison between the present compound and the two mentioned above is not extremely meaningful because of the different number of non-RE atoms, one can use scaling to compare these different systems. If we compare the susceptibility/atom (or susceptibility/volume), then $LaAu_2In_4$ has comparable paramagnetic susceptibility compared to the first compound and smaller susceptibility compared with the second compound.

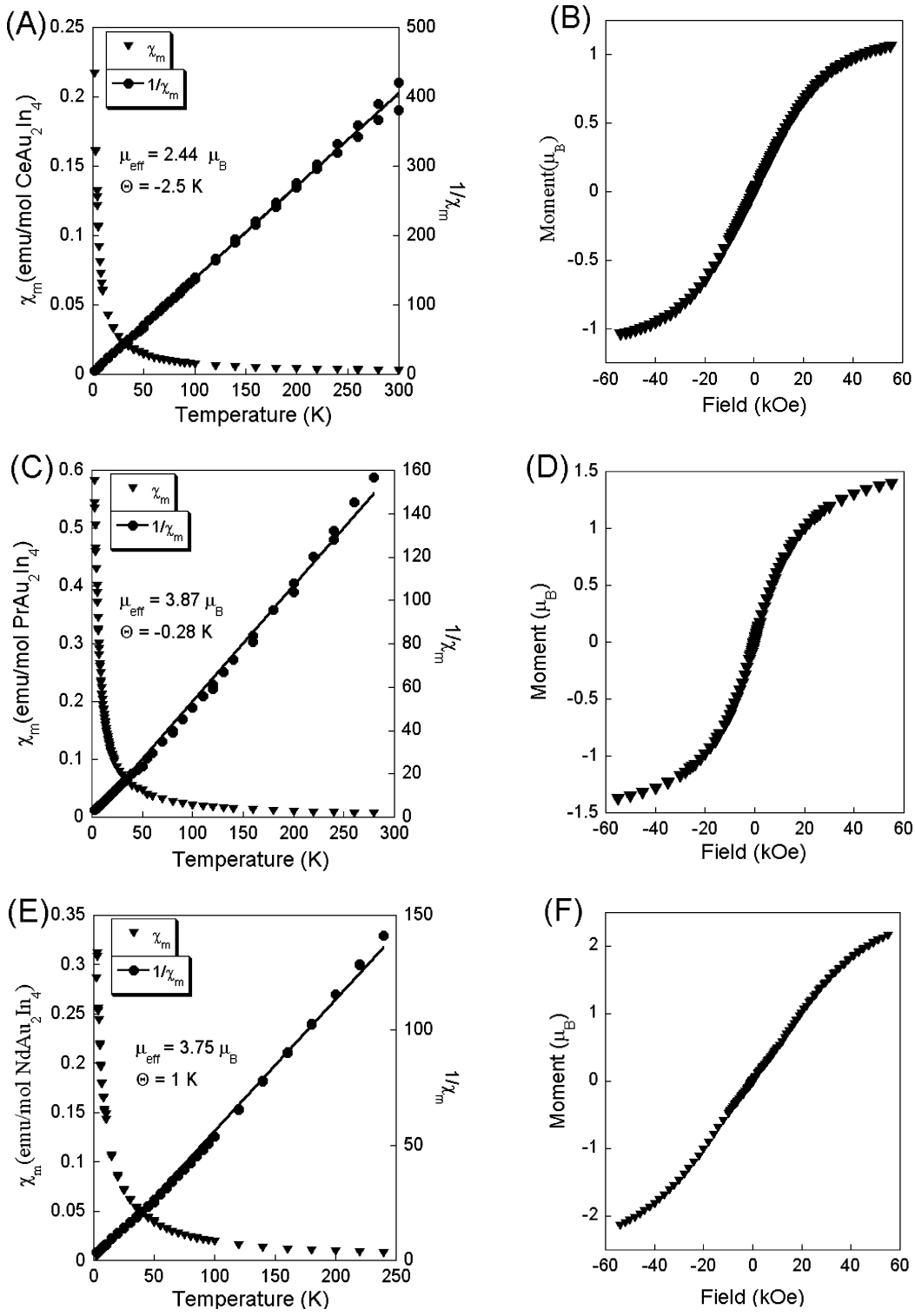

Figure 6. (A) Magnetic susceptibility for $CeAu_2In_4$ collected with an applied field of 500 Oe. (B) Magnetization data for $CeAu_2In_4$ collected at 2 K. (C) Magnetic susceptibility data for $PrAu_2In_4$ collected with an applied field of 2 kOe. (D) Magnetization data for $PrAu_2In_4$ collected at 2 K (E) Magnetic susceptibility data for $NdAu_2In_4$ collected with an applied field of 2 kOe. (F) Magnetization data for $NdAu_2In_4$ collected at 2 K.

trend continues out to 55 kOe. The moment reaches a value of about 1.4 μ_B at 55 kOe, which is about half of the value anticipated for the fully saturated moment of a Pr^{3+} ion.

$NdAu_2In_4$. The temperature-dependent susceptibility data for $NdAu_2In_4$ is shown in Figure 6E. As was the case with the other analogues, there is no magnetic ordering observed down to 2 K, and the inverse susceptibility data obeys the Curie−Weiss law from 300 to 2 K. The effective magnetic moment was 3.75 μ_B and agrees quite well with the calculated moment for an Nd^{3+} ion, which is 3.6 μ_B. The Weiss constant is small and positive ($\theta = 1.0$ K), indicating weak ferromagnetic interactions between the ions.

The magnetization curve for $NdAu_2In_4$ at 2 K is linear up to approximately 40 kOe (Figure 6F). Above this field. the slope of the curve changes slightly and becomes shallower but continues to be linear up to the highest applied field of 55 kOe. $NdAu_2In_4$ showed no sign of saturation and only reached 2.1 μ_B at the highest applied field. This is less than two-thirds the value expected for a saturated system.

The magnetic susceptibility results suggest that the RE atom is the only species that contributes to the paramagnetic susceptibility (except for La) and that the remaining atoms along with the valence electrons of RE atoms are associated with weakly temperature-independent paramagnetic susceptibility. We can therefore regard these compounds as polar intermetallics.

The absence of ordering down to 2 K in all analogues indicates that the moments of the RE atoms are weakly coupled magnetically. In $REAu_2In_4$, the RE atoms are separated by too great a distance (4.61 to 4.68 Å) for direct magnetic exchange to be effective. The indirect exchange in metallic systems is the Ruderman−Kittel−Kasuya−Yosida (RKKY) mechanism[70,71] in which magnetic coupling is mediated by the conduction electrons. The lack of ordering down to 2 K also suggests a very weak RKKY coupling. Weak RKKY coupling may occur if the electronic DOS near the Fermi energy is very small (see below).

Electronic Structure Calculations. To obtain more insight into the bonding in $LaAu_2In_4$, its structural stability, and the electronic DOS near the Fermi energy (E_f) electronic band structure calculations were performed on the La analogue. In the other compounds with f electrons (RE = Ce, Pr, Nd), we expect some of the generic features such as In−In bonding, the effect of Au d electrons on the bonding, and the DOS near E_f to be similar. We started out with experimental lattice parameters and after allowing for relaxation of the unit-cell shape and ionic positions, we found that the lattice parameters did not change appreciably. However, slight shifts of the atoms resulted in a reduction in the total energy of 3.84 meV/f.u. (f.u. = $LaAu_2In_4$). This relaxation energy is small, suggesting that the experimental and theoretical structures are quite close. The internal atomic relaxations are about 0.1%.

The total DOS up to ~1 eV above E_f (at 0 eV) obtained from both LAPW and PAW calculations (without SOI) are shown in Figure 7. The two calculations agree extremely well, as they should. The main features of the total DOS are two large peaks centered around −5 and −6.25 eV overlapping a broad band spanning from ca. −9.75 eV to well above E_f. The partial DOS associated with La, Au(1), In(1), and In(2) atoms obtained from the LAPW calculations without SOI are shown in Figure 8. The La f states are centered ~3 eV above E_f and contribute very little to the occupied states. There is only a small amount of La d state below E_f. Thus, La acts primarily as a 3+ ion. The Au d states dominate the DOS in the range ca. −3 to −7.6 eV (the two peaks separated by ~1.5 eV correspond to crystal-field splitting) and are

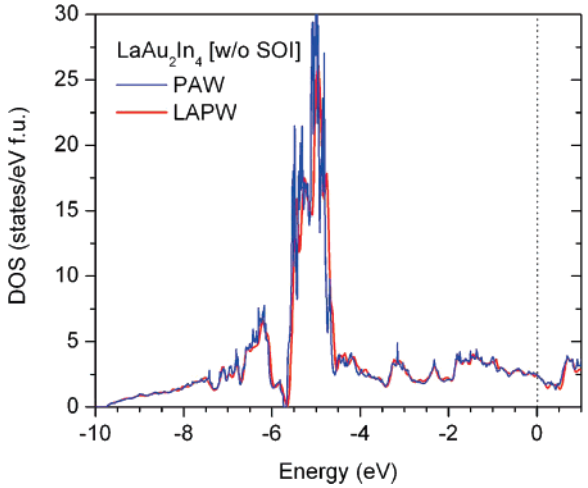

Figure 7. Total DOS of $LaAu_2In_4$ obtained in PAW and LAPW calculations without spin−orbit interaction (SOI). The Fermi level (E_f) is at 0 eV.

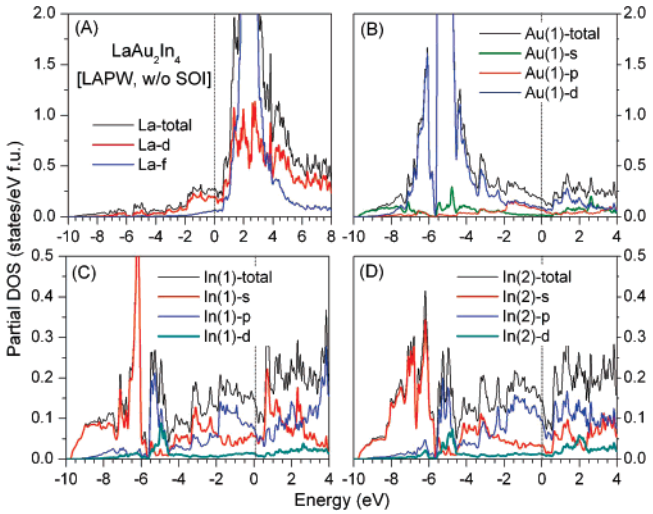

Figure 8. Partial DOS for (A) La, (B) Au(1), (C) In(1), and (D) In(2) obtained in LAPW calculations without SOI. The Fermi level (E_f) is at 0 eV.

filled. About half of the Au s states also lie below E_f, consistent with Au being the most electronegative of the three elements present in this compound. The In s and In p states contribute to the broad conduction band. The largest contribution to the total DOS at E_f comes from the s and p states of In with a small amount of Au p and d and La d character.

There is a significant difference in the partial s orbital DOS associated with In(1) and In(2). This difference was further explored by calculating the ELF.[59] In order to see the effect of SOI on the DOS, particularly near E_f, we also carried out PAW calculations with and without SOI. We found that the SOI had negligible effect on the DOS near the E_f. However, there is a large rearrangement in the DOS between −4 and −7 eV because of the splitting of the Au d states (Figure 9).

The nature of the bonding between constituent atoms in the compound was explored with the ELF.[59] The ELF values lie between 1 and 0; it is 0.5 for a homogeneous charge distribution. In Figure 10, we show the isosurface associated

(70) Kasuya, T. *Prog. Theoret. Phys.* **1956**, *16* (1), 45−57.
(71) Mitchell, A. H. *Phys. Rev.* **1957**, *105* (5), 1439−1444.

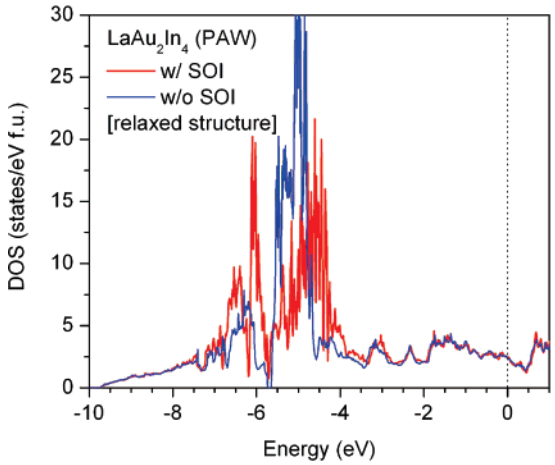

Figure 9. Total DOS of $LaAu_2In_4$ obtained in PAW calculations with and without SOI. The Fermi level (E_f) is at 0 eV.

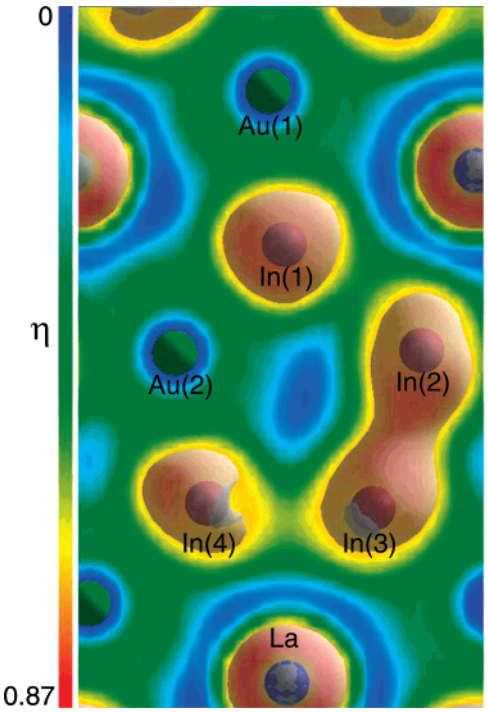

Figure 10. ELF for $LaAu_2In_4$ in the (010) plane obtained in PAW calculations. The isosurface is associated with the ELF value $\eta = 0.7$. The blue spheres are La, the green spheres are Au, and the brown spheres are In atoms.

with a given ELF value ($\eta = 0.7$). We can clearly see the difference in the bonding between four different inequivalent In atoms, In(1) through In(4). A stronger bond is suggested by the ELF between In(2) and In(3) than between In(1)−In(2) and In(3)−In(4). If we go to a lower ELF value ($\eta = 0.5$), In(2)−In(3)−In(4) form a connected trimer and In(1) is isolated. These results are consistent with the observed bond lengths between In(1)−In(2) (3.129(2) Å), In(2)−In(3) (2.987(2) Å), and In(3)−In(4) (2.988(2) Å).

We find that the DOS decreases slowly near E_f and reaches a minimum at about 0.5 eV above E_f. There is no evidence of a pseudogap, and therefore, we are not dealing with a semimetal. To check whether the theoretical electronic structure can explain the observed weak Pauli paramagnetism of $LaAu_2In_4$, we estimated the Pauli susceptibility from the total DOS at E_f using the relation[72]

$$\chi_{Pauli} = \mu_B{}^2 N(E_f)$$

where μ_B is the Bohr magneton and $N(E_f)$ is the DOS at the Fermi level. Using the calculated DOS of 2.5 states/eV f.u., we find the theoretical value of Pauli susceptibility to be 0.8×10^{-4} emu/mol, a factor of 2 smaller than that of the experiment ($\sim 1.66 \times 10^{-4}$ emu/mol La). A simple way to account for this discrepancy is to include the effect of electron−electron interaction beyond that included in the single-particle DOS calculation. It is known that χ_{Pauli} is exchange enhanced.[72] A factor value of 2 for exchange enhancement is not unreasonable. We have to also take into account, however, the diamagnetic and orbital paramagnetic contributions associated with the valence (conduction) electrons. A numerical estimate of these two contributions for this rather non-free-electron-like system is beyond the scope of the present work, but they generally tend to cancel each other.

Concluding Remarks

This work shows the ability of molten indium to stabilize complex intermetallic compounds as well-formed crystals. The compounds $REAu_2In_4$ (RE = La, Ce, Pr, Nd) exhibit In−In bonding, and they are defined as polyindides in a new structure type. In view of the large number of ternary phases already described in this system, the discovery of $REAu_2In_4$ is particularly interesting and underscores the value of using liquid In as a medium for exploratory intermetallic synthesis. The reactions in molten indium proceeded at a much faster rate than the direct combination reactions run at the same temperature.

The magnetic susceptibility of $LaAu_2In_4$ is small and temperature-independent, indicating Pauli paramagnetic behavior. The other members do not order magnetically and follow the Curie−Weiss law with small Weiss constants. These facts point to these compounds being poor metals. The latter quality can be traced to the low DOS at the Fermi level suggested from DFT calculations. The calculations for $LaAu_2In_4$ indicate that the bands near the Fermi level are formed primarily from In s and p states, justifying the polyindide picture of these compounds. The La atoms donate their valence electrons mainly to the indium−gold network. The bonding between different In atoms is nonuniform, and there is a slight tendency of dimerization between In(2) and In(3).

Acknowledgment. Financial support from the Department of Energy (Grant No. DE-FG02-99ER45793) is gratefully acknowledged. Calculations were partly performed at the High Performance Computing Center (HPCC) of Michigan State University.

Supporting Information Available: DTA plots of $LaAu_2In_4$ in PDF format and one CIF file. This material is available free of charge via the Internet at http://pubs.acs.org.

IC700633B

(72) Ashcroft, N. W.; Mermin, N. D. *Solid State Physics*; Saunders College Publishing, 1976.